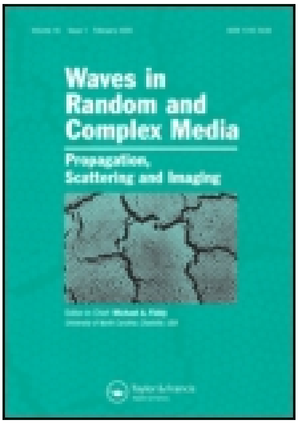

Waves in Random and Complex Media
Publication details, including instructions for authors and subscription information:
http://www.tandfonline.com/loi/twrm20

A study of SH-SAW propagation in cubic piezomagnetics for utilization in smart materials

A.A. Zakharenko [a]
[a] International Institute of Zakharenko Waves (IIZWs) 660037, Krasnoyarsk-37, 17701, Krasnoyarsk, Russia
Version of record first published: 09 Oct 2012.

To cite this article: A.A. Zakharenko (2012): A study of SH-SAW propagation in cubic piezomagnetics for utilization in smart materials, Waves in Random and Complex Media, 22:4, 488-504

To link to this article: http://dx.doi.org/10.1080/17455030.2012.727042

Waves in Random and Complex Media
Vol. 22, No. 4, November 2012, 488–504

A study of SH-SAW propagation in cubic piezomagnetics for utilization in smart materials

A.A. Zakharenko*

International Institute of Zakharenko Waves (IIZWs) 660037, Krasnoyarsk-37, 17701, Krasnoyarsk, Russia

(*Received 9 March 2012; final version received 30 August 2012*)

This theoretical investigation provides characteristics of shear-horizontal surface acoustic waves (SH-SAWs) in piezomagnetic cubic monocrystals. The wave characteristics for various cubic piezomagnetics such as Alfenol, Terfenol-D, Metglas, $NiFe_2O_4$, etc., with the coefficient of magnetomechanical coupling (CMMC) $K_m^2 < 1/3$ and $K_m^2 < 1/3$ are studied. Knowledge of properties of cubic piezomagnetics is beneficial to the design of smart devices, sensors, and actuators, as well as applications in non-destructive testing. Also, the obtained results allow us to choose apt materials to constitute piezomagnetic/piezoelectric laminate composites in the microwave technology.

1. Introduction

Shear-horizontal surface acoustic waves (SH-SAWs), also called surface Bleustein–Gulyaev (BG) waves, were first discovered in transversely-isotropic piezoelectrics in 1968–1969 [1,2]. In [3], Al'shits et al. reported a qualitative investigation on the existence of SH-SAWs in piezoelectrics and piezomagnetics. According to [3], the piezomagnetic effect and the piezoelectric effect can be described in the same way. As a result, as in the transversely-isotropic piezoelectrics, the surface BG-waves can also propagate in transversely-isotropic piezomagnetics. However, the surface BG-waves cannot exist in cubic piezoelectrics (hence, in cubic piezomagnetics). This was stated in a recent paper [4] by Gulyaev (the co-discoverer of the surface BG-wave) and Hickernell published in 2005. This conclusion was also confirmed in [5]. As for cubic piezoelectrics and cubic piezomagnetics, the ultrasonic surface Zakharenko waves (USZWs) [5] can exist in cubic monocrystals. Based on the results of [5], all cubic piezomagnetics in contrast to the transversely-isotropic materials can be divided into two groups: the first group includes cubic piezomagnetics with $K_m^2 < 1/3$ and the second is for cubic piezomagnetics with $K_m^2 < 1/3$, where K_m^2 is the coefficient of the magnetomechanical coupling (CMMC). For $K_m^2 < 1/3$, the USZW velocity can significantly differ from the BG-wave velocity, V_{BG}, compared with the difference between the bulk wave velocity V_{tm} and the V_{BG}, and the second 'latent SAW'

*Email: aazaaz@inbox.ru

ISSN 1745–5030 print/ISSN 1745–5049 online

http://dx.doi.org/10.1080/17455030.2012.727042
http://www.tandfonline.com

solution with the value of V_{aKm} (see below) is always found. For $K_m^2 < 1/3$, the USZW velocity is situated slightly below the V_{aKm}, and the difference between the USZW velocity and the V_{BG} may reaches a very large value (even $\sim$100 m/s) according to the results for cubic piezomagnetics Galfenol and Terfenol-D [6]. In the case of the magnetic potential $\psi = 0$ in the magnetic boundary conditions, the USZW velocity for cubic piezomagnetics [6,7] coincides with the V_{BG}. To date, little is known about the SH-SAW characteristics in cubic piezomagnetics and even in transversely-isotropic piezomagnetics.

Also, it is worth noting that some attempts [8–11] to analytically and numerically find the surface SH-waves in crystals with cubic symmetry occurred before paper [4] was published in 2005 by Gulyaev and Hickernell. However, these attempts did not reveal the significant differences of the surface SH-wave propagation in cubic crystals described above from that in the transversely-isotropic materials. On the contrary, these studies [8–11] presented their results in such a way that the surface SH-wave propagation in cubic crystals is similar to that in the transversely-isotropic materials with none of the differences briefly described above in this introductory section. This is cannot actually be trusted and looks like fake or incorrect results. As a result, Academician Gulyaev (the co-discoverer of the surface BG-waves) and Hickernell (who worked with the other co-discoverer) stated in [4] that the surface BG-waves cannot exist in cubic piezoelectrics (hence, in cubic piezomagnetics.).

This paper studies the wave characteristics of various cubic piezomagnetics for utilization of the materials with the cubic symmetry in smart composite materials. Like the transversely-isotropic composite materials [12], cubic composite materials can also reveal their uniqueness. Note that some transversely-isotropic materials are frequently treated as pseudo-cubic materials. It is natural that a piezomagnetic material is a suitable pair component for a piezoelectric material to study magnetoelectric coupling. In recent topical reviews [13–15], more than 300 references on the subject were documented, in particular some pioneer works [16–20] about piezomagnetic–piezoelectric composite materials and the magnetoelectric effect. References [21–27] investigated the problem of the magnetoelectric effect in laminated composites. Recent review papers [28,29] have discussed various device applications when piezoelectrics and piezomagnetics are combined together to form, for example, multi-layered structures. In 2009, review [28] particularly listed the applications of Fe-containing materials in microwave passive devices such as phase shifters, circulators, filters, isolators, and resonators. In 2010, review [29] also focused on potential device applications for the composites of magnetostrictive and piezoelectric phases such as magnetic-field sensors, dual electric-field- and magnetic-field-tunable microwave and millimeter-wave devices, and miniature antennas. It is noted that this research arena is rapidly developed and reviews on the subject can be published every year. Also, of much interest is a study of interfacial wave propagation in piezomagnetic–piezoelectric laminated composites [7,30]. Knowledge of wave properties of piezomagnetic cubic monocrystals can guarantee a right choice of materials for a study of interfacial waves in piezomagnetic–piezoelectric composites. The results of this paper can help to resolve some current problems concerning utilization of cubic piezomagnetics in the layered composites. The following section provides the theory for the SH-SAW propagation in the cubic piezomagnetics.

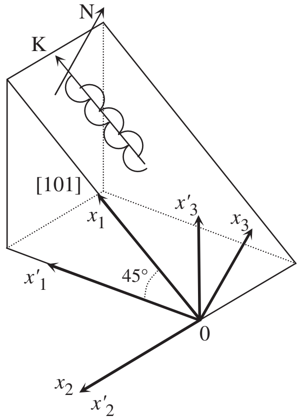

Figure 1. The SH-SAW propagation along direction [101] for a piezomagnetic cubic monocrystal. **K** is the wave vector in the direction of wave propagation and **N** is the vector of surface normal.

2. Theory of SH-SAW propagation

The piezomagnetic SH-SAWs with the anti-plane polarization can propagate along the crystal surface in direction [101] perpendicular to an even-order symmetry axis. The used rectangular coordinate system $\{x'_1 = X,\ x'_2 = Y,\ x'_3 = Z\}$ is shown in Figure 1, in which the crystallographic coordinates X, Y, and Z are directed along the fourth-order symmetry axes of a piezomagnetic cubic crystal of classes $m3m$ and 432 or along the second-order symmetry axes of a cubic piezomagnetics of class $m3$ [31,32]. Direction [101] is obtained by 45°-rotation around the x'_2-axis. According to [3], the theoretical description of wave propagation in the cubic piezomagnetics is similar to that for the cubic piezoelectrics. The constitutive equations for piezomagnetics can be expressed in terms of the magnetic field H and the strains τ related to the mechanical displacements U_j as follows: $\tau_{ij} = (\partial U_i/\partial x_j + \partial U_j/\partial x_i)/2$ [33]. The governing mechanical equilibrium is $\partial\sigma_{ij}/\partial x_j = 0$ and the governing magnetostatic equilibrium is $\partial B_i/\partial x_i = 0$, where σ_{ij} and B_i are the stress tensor and magnetic flux, respectively.

A piezomagnetic medium possesses the elastic stiffness constants C_{ijkl}, piezomagnetic coefficients h_{ijk}, constant strain magnetic permeability coefficients μ_{ij}, and mass density ρ. Treating the linear case, constitutive relations read:

$$\sigma_{ij} = C^H_{ijkl}\tau_{kl} - h_{ijm}H_m, \tag{1}$$

$$B_m = h_{mij}\tau_{ij} + \mu^\tau_{mn}H_n, \tag{2}$$

with the following thermodynamic definitions for the material constants:

$$C^H_{ijkl} = \left(\frac{\partial\sigma_{ij}}{\partial\tau_{kl}}\right)_H, \tag{3}$$

$$h_{mij} = h_{ijm} = -\left(\frac{\partial\sigma_{ij}}{\partial H_m}\right)_\tau = \left(\frac{\partial B_m}{\partial\tau_{ij}}\right)_H, \tag{4}$$

$$\mu^{\tau}_{mn} = \left(\frac{\partial B_m}{\partial H_n}\right)_{\tau}. \tag{5}$$

In Equations (1)–(5), the indices i, j, k, l, m, and n run from 1 to 3. Also, σ_{ij} and τ_{ij} are the stress and strain tensor components, respectively. $H_m = -\partial\psi/\partial x_m$ (ψ is the magnetic potential) are the components of the magnetic field. According to the Voigt notation, C_{ijkl}, h_{ijm}, and μ_{mn} can be written as 6×6, 3×6, and 3×3 matrices standing for the elastic, piezomagnetic, and magnetic tensors, respectively.

In the quasi-static approximation, the equations of motion of an elastic medium can be written as follows:

$$\frac{1}{\rho}\frac{\partial\sigma_{ij}}{\partial x_j} - \frac{\partial^2 U_i}{\partial t^2} = 0, \tag{6}$$

and the magnetostatics equation reads

$$\frac{\partial B_i}{\partial x_j} = 0. \tag{7}$$

In Equation (6), the second term represents the second derivative of the mechanical displacement components U_i with respect to time t. Using Equations (1)–(7), one can write the coupled equations of motion for a piezomagnetic medium in the following form:

$$\rho\frac{\partial^2 U_i}{\partial t^2} = C_{ijkl}\frac{\partial^2 U_l}{\partial x_j \partial x_k} + h_{kij}\frac{\partial^2 \psi}{\partial x_j \partial x_k}, \tag{8}$$

$$0 = h_{ijk}\frac{\partial^2 U_k}{\partial x_i \partial x_j} - \mu_{ij}\frac{\partial^2 \psi}{\partial x_i \partial x_j}. \tag{9}$$

If one denotes the displacement component ψ as U_4, solutions of homogeneous partial differential Equations (8) and (9) of the second order can be expressed in terms of the following plane wave form: $U_{1,2,3,4} = U^0_{1,2,3,4}\exp[\mathrm{j}\,(k_1x_1 + k_2x_2 + k_3x_3 - \omega t)]$ where U^0_i $(i=1,2,3)$ and $U^0_4 = \psi^0$ are the initial amplitudes; ω is the angular frequency and $\mathrm{j} = (-1)^{1/2}$. The wavevector $\{k_1, k_2, k_3\} = k\{n_1, n_2, n_3\}$ where $\{n_1, n_2, n_3\}$ is the directional cosine vector. Also, $\{x_1, x_2, x_3\}$ are the components of the real space vector.

A further simplification of Equations (8) and (9) for the studied case can be achieved by leaving only equations associated with SH-SAWs. That is, for SH-SAWs propagating in the direction [101], one has

$$\rho\frac{\partial^2 U}{\partial t^2} = C\left(\frac{\partial^2 U}{\partial x_1^2} + \frac{\partial^2 U}{\partial x_3^2}\right) - h\frac{\partial^2 \psi}{\partial x_1^2} + h\frac{\partial^2 \psi}{\partial x_3^2}, \tag{10}$$

$$0 = -h\frac{\partial^2 U}{\partial x_1^2} + h\frac{\partial^2 U}{\partial x_3^2} - \mu\left(\frac{\partial^2 \psi}{\partial x_1^2} + \frac{\partial^2 \psi}{\partial x_3^2}\right), \tag{11}$$

because of the fact that $C_{ijkl} \to C_{44} = C_{66} = C$, $h_{ijm} \to h_{16} = -h_{34} = h$ and $\mu_{mn} \to \mu_{33} = \mu_{11} = \mu$. In Equations (10) and (11), the mechanical displacement component $U = U_2$

is directed along the x_2-axis (see Figure 1):

$$U_{2,4} = U_{2,4}^0 \exp\left[jk\left(n_1 x_1 + n_3 x_3 - V_{ph} t\right)\right], \tag{12}$$

where the phase velocity V_{ph} is defined by $V_{ph} = \omega/k$ (k is the wavenumber in the direction of wave propagation.) Note that the directional cosines in Equation (12) are defined as follows: $n_1 \equiv 1$, $n_2 \equiv 0$ and $n_3 = n_3$.

Coupled Equations (8) and (9) can be also written in a tensor form. In this form, the GL-components of the tensor in the Green–Christoffel equation are written as follows: $(\mathrm{GL}_{sw} - \delta_{sw}\rho V_{ph})U_s = 0$ [6,34] where s and w run from 1 to 4, δ_{sw} is the Kronecker delta for $s < 4$ and $w < 4$, $\delta_{44} = 0$, $U_s = \{U_1, U_2, U_3, \psi\}$. In the simplified case of Equation (10) and (11), the equations of motion can be written in the well-known tensor form, using the corresponding components of the GL-tensor: $\mathrm{GL}_{22} = Cm$, $\mathrm{GL}_{24} = \mathrm{GL}_{42} = h(m-2)$ and $\mathrm{GL}_{44} = -\mu m$ with $m = 1 + n_3^2$. Therefore, the following system of two homogeneous equations for pure SH-waves can be written as:

$$\begin{pmatrix} \mathrm{GL}_{22} - C(V_{ph}/V_{t4})^2 & \mathrm{GL}_{24} \\ \mathrm{GL}_{42} & \mathrm{GL}_{44} \end{pmatrix} \begin{pmatrix} U_2^0 \\ \psi^0 \end{pmatrix} = \begin{pmatrix} 0 \\ 0 \end{pmatrix}, \tag{13}$$

where $V_{t4} = (C_{44}/\rho)^{1/2}$. Setting the determinant of the coefficient matrix in Equation (13) equal to zero, a suitable phase velocity V_{ph} satisfying the mechanical and magnetic boundary conditions discussed in the following section can be determined. Once V_{ph} is determined, non-trivial functions $U_2^0(V_{ph})$ and $\phi^0(V_{ph})$ can also be obtained to satisfy $\psi^0 = \mathrm{GL}_{42}$ and $U_2^0 = -\mathrm{GL}_{44}$. It is worth noting that for the surface Bleustein–Gulyaev waves for transversely-isotropic piezomagnetics, the GL_{24} and GL_{42} components are written as follows: $\mathrm{GL}_{24} = \mathrm{GL}_{42} = hm$.

Expanding the determinant of the coefficient matrix in Equation (13), one can obtain the following quadratic equation:

$$\left(1 + K_m^2\right)\mathrm{m}^2 - Dm + 4K_m^2 = 0, \tag{14}$$

with

$$D = \left(\frac{V_{ph}}{V_{t4}}\right)^2 + 4K_m^2. \tag{15}$$

Two polynomial roots $m^{(1,2)}$ of Equation (14) can be written as follows

$$m^{(1,2)} = \frac{D \pm \sqrt{D^2 - 16K_m^2\left(1 + K_m^2\right)}}{2\left(1 + K_m^2\right)}. \tag{16}$$

Therefore, four polynomial roots (eigenvalues) of Equation (13) as functions of the appropriate phase velocity V_{ph} are:

$$n_3^{(1,2,3,4)} = \pm\sqrt{-1 + m^{(1,2)}}. \tag{17}$$

For each eigenvalue $n_3^{(p)}$, the corresponding eigenvector is also obtained in the following form: $(U_2^{(p)}, \psi^{(p)})$ where $p = 1, 2, 3, 4$. In Equations (14)–(16), the coefficient K_m^2 is called the coefficient of the magnetomechanical coupling (CMMC):

$$K_m^2 = h^2/(C\mu). \tag{18}$$

From Equation (17), it can be inferred that complex roots may occur if $m^{(1,2)} < 1$. This fulfills when the V_{ph} is lower than some velocity V_{aKm} obtained by solving the following expression from Equation (16): $D^2 - 16K_m^2(1 + K_m^2) = 0$ where V_{aKm} is defined by

$$V_{aKm} = a_{Km} V_{t4}, \tag{19}$$

with

$$a_{Km} = 2\sqrt{K_m\left(1 + K_m^2\right)^{1/2} - K_m^2}. \tag{20}$$

Note that the speed V_{tm} of the bulk SH-wave is given by the following well-known formula:

$$V_{tm} = V_{t4}\left(1 + K_m^2\right)^{1/2}. \tag{21}$$

Indeed, only complex polynomial roots of Equation (17) exist when $V_{ph} < V_{aKm}$. Following [5,6], within the phase velocity interval such that $V_{tm} > V_{ph} > V_{aKm}$ only imaginary roots of Equation (17) can exist for a small value of the CMMC $K_m^2 < 1/3$, but all polynomial roots of Equation (17) become real for a large value of $K_m^2 > 1/3$. It is noted that in order to ensure wave decaying behavior away from the surface or interface, only complex or imaginary roots with negative imaginary parts are chosen. This corresponds to the negative values of the x_3-axis of the work coordinate system $\{x_1, x_2 = x_2', x_3\}$ shown in Figure 1.

For free space, Laplace's equation of type $\Delta\psi = 0$ is written in the following form: $(k_1^2 + k_3^2)\psi_0 = 0$ where μ_0 is the magnetic constant for a vacuum. The magnetic potential for the free space is then represented by $\psi_0 = F^{(0)}\exp(-k_1 x_3) \times \exp[j(k_1 x_1 - \omega t)]$ where $k_1 > 0$, implying that the potential ψ_0 must decrease with increase in $x_3 > 0$ (see Figure 1).

3. Mechanical and magnetic boundary conditions

The mechanical and magnetic boundary conditions of a studied piezomagnetics which occupies the half-space $x_3 < 0$ (see Figure 1) must be satisfied. It is often assumed that the magnetic boundary condition is either magnetically closed ($B_3 = 0$) or magnetically open ($\psi = 0$) surface at $x_3 = 0$. The realization of the magnetic boundary conditions is described in [3]. The mechanical boundary condition for the problem in question is $\sigma_{32} = 0$ at $x_3 = 0$, where

$$\sigma_{32} = F^{(1)}\left[Ck_3^{(1)}U_2^{(1)} + hk_3^{(1)}\psi^{(1)}\right] + F^{(2)}\left[Ck_3^{(2)}U_2^{(2)} + hk_3^{(2)}\psi^{(2)}\right] \tag{22}$$

is the normal stress component. In addition, the magnetic flux and the magnetic potential are expressed, respectively, as follows:

$$B_3 = F^{(1)}\left[hk_3^{(1)}U_2^{(1)} - \mu k_3^{(1)}\psi^{(1)}\right] + F^{(2)}\left[hk_3^{(2)}U_2^{(2)} - \mu k_3^{(2)}\psi^{(2)}\right], \tag{23}$$

$$B_3^f = -F^{(0)}\psi_0^f jk_1\mu_0; \tag{24}$$

and

$$\psi = F^{(2)}\psi^{(2)} + F^{(2)}\psi^{(2)}, \tag{25}$$

$$\psi^f = F^{(0)}\psi_0^f, \tag{26}$$

where a quantity with the superscript f specifies the one corresponding to the free space.

For the mechanically free and magnetically closed surface, using Equations (23)–(26), one gets the following two homogeneous equations:

$$\begin{pmatrix} Ck_3^{(1)}U_2^{(1)} + hk_3^{(1)}\psi^{(1)} & Ck_3^{(2)}U_2^{(2)} + hk_3^{(2)}\psi^{(2)} \\ hk_3^{(1)}U_2^{(1)} - (\mu k_3^{(1)} - \mathrm{j}\mu_0 k_1)\psi^{(1)} & hk_3^{(2)}U_2^{(2)} - (\mu k_3^{(2)} - \mathrm{j}\mu_0 k_1)\psi^{(2)} \end{pmatrix}\begin{pmatrix} F^{(1)} \\ F^{(2)} \end{pmatrix} = 0. \tag{27}$$

In contrast, for the mechanically free and magnetically open surface ($\psi = 0$), the above-derived equation is replaced by

$$\begin{pmatrix} Ck_3^{(1)}U_2^{(1)} + hk_3^{(1)}\psi^{(1)} & Ck_3^{(2)}U_2^{(2)} + hk_3^{(2)}\psi^{(2)} \\ \psi^{(1)} & \psi^{(2)} \end{pmatrix}\begin{pmatrix} F^{(1)} \\ F^{(2)} \end{pmatrix} = 0. \tag{28}$$

The complete mechanical displacement U_2^{Σ} and magnetic potential $\psi^{\Sigma} = U_4^{\Sigma}$ can be expressed in the plane wave form as follows:

$$U_{2,4}^{\Sigma} = \sum_{p=1,2} F^{(p)} U_{2,4}^{0(p)} \exp\left[\mathrm{j}k\left(n_1 x_1 + n_3^{(p)} x_3 - V_{ph} t\right)\right]. \tag{29}$$

For Equations (27) and (28), the corresponding weight functions $F^{(1)}$ and $F^{(2)}$ can be also found. It is very interesting that in the case of direction [101] of wave propagation in the cubic materials, two equal eigenvalues $n_3^{(1)} = n_3^{(2)}$ can exist for the phase velocity $V_{ph} = V_{aKm}$. The equal eigenvalues result in the same eigenvectors $(U_2^{0(1)}, \Psi^{0(1)})$ and $(U_2^{0(2)}, \Psi^{0(2)})$ and hence $F^{(1)} = -F^{(2)}$. It is obvious that for this case the weight factors $F^{(1)} = -F^{(2)}$ will zero the values of U_2^{Σ} and $\psi^{\Sigma} = U_4^{\Sigma}$ in Equation (29). Therefore, it is possible to state that one copes here with a 'latent' characteristic in Equation (29) for $V_{ph} = V_{aKm}$ because such 'latent SAW' will have zero penetration depth due to $U_2^{\Sigma} = \psi^{\Sigma} = 0$. On the other hand, unequal eigenvalues $n_3^{(1)}$ and $n_3^{(2)}$ result in different eigenvectors $(U_2^{0(1)}, \Psi^{0(1)})$ and $(U_2^{0(2)}, \Psi^{0(2)})$ and hence non-zero U_2^{Σ} and $\psi^{\Sigma} = U_4^{\Sigma}$ in Equation (29). For the case of $U_2^{\Sigma} = \psi^{\Sigma} = 0$, it is thought that the 'latent SAW' with $V_{ph} = V_{aKm}$ for the case of $K_m^2 < 1/3$ must be experimentally verified because the ultrasonic surface Zakharenko waves are found slightly below the velocity V_{aKm} for the case of $K_m^2 > 1/3$. Therefore, it is possible here to describe an instability problem for both velocities V_{tm} and V_{aKm} leading to SAW propagation along the crystal surface. Also, it is possible to mention the fact that some elements of crystal symmetry (screw axis or glide reflection) can be broken near the surface. It is also noted that the solution V_{aKm} does not exist when the surface Bleustein–Gulyaev waves are studied in the transversely-isotropic piezomagnetics. This is an additional significant difference for finding the BG-waves in the transversely-isotropic piezomagnetics and the USZWs in cubic piezomagnetics. However, for the case of $\psi = 0$, the USZW velocity coincides with the BG-wave velocity.

4. Material properties of cubic piezomagnetics

The material constants of some cubic piezomagnetics of ceaseless interest in utilization in various technical devices are listed in Table 1. In general, the elastic compliances S_{ij}, piezomagnetic constants q (m/A), and constant stress magnetic permeability μ^{σ} are given in almost all works. Notwithstanding, Table 1 lists the elastic stiffness constant C_{44}, piezomagnetic coefficient h_{16} (Tesla), and constant strain magnetic permeability μ_{11}. According to [31,32], the elastic stiffness constant C_{44} and the compliance S_{44} are related by $C_{44} = 1/S_{44}$ for all cubic and hexagonal classes. The piezomagnetic coefficient $h_{16} = h$ can be calculated with the following formula, using Equation (18): $h = K_m\sqrt{C\mu}$. Also, the magnetic permeability μ^{σ} at the constant stress and the constant strain permeability μ^{τ} are related by $\mu^{\tau} = \mu^{\sigma}(1 - K_m^2)$. It is emphasized that this expression is only valid for linear systems and significant corrections are necessary in order to extend this formula to the full nonlinear regime.

The elastic stiffness constants C_{44} and the mass densities ρ for Ni were borrowed from [35]. C_{44} for Alfenol is written following [36,37]. The piezomagnetic and magnetic properties of Ni, Alfenol, Terfenol-D(1), and Ferroxcube 7A1 listed in Table 1 were borrowed from [21,38,39]. The mass densities ρ for Terfenol-D(1) and Metglas 2605 are also listed in [14]. The static coefficients of magnetomechanical coupling (CMMC) K_m^2 for Ni, Alfenol, Terfenol-D(1), Ferroxcube 7A1, and Metglas 2605 were also reported in [39–42]. It is also noticed that the piezomagnetic coefficient for Metglas (FeBSiC) discussed in [43] is several times smaller than that given in [39]. The material properties of Terfenol-D(2) and Terfenol-D(3) read according to [44], which demonstrated a set of different material constants for Terfenol-D. Different material properties of Terfenol-D(2) and Terfenol-D(3) are chosen, which, respectively, correspond to a small value of K_m^2 and a very large value of K_m^2 even for Terfenol-D. Note that piezomagnetics Metglas and Terfenol-D are roughly equivalent to piezoelectrics PVDF and PZT. It is also noted that piezomagnetics Ni and Alfenol are roughly equivalent to piezoelectrics quartz.

Also, the elastic stiffness C_{44}, magnetic permeability μ_{11}, and mass density ρ are used the same as those for nickel ferrite $NiO \cdot Fe_2O_3$ ($NiFe_2O_4$) and zinc-doped nickel ferrite $(NiO)_{0.8}(ZnO)_{0.2}Fe_2O_3$ ($Ni_{0.8}Zn_{0.2}Fe_2O_4$); see [14,45–47]. However, the piezomagnetic coefficient for $NiFe_2O_4$ is 20% to 30% smaller than that for zinc-doped nickel ferrite. These material constants give very small values of K_m^2 for both ferrites. Like cobalt ferrite, nickel ferrite is an alternative piezomagnetic material, which exhibits nearly ideal interface coupling [13]. Also, the magnetoelectric voltage coefficient of $NiFe_2O_4$ is increased by a factor of 1.5 for 20% substitution of Ni by Zn. In [48,49], the principal motivation was to investigate the overall coupled magnetic–dielectric properties of simple particulate $NiFe_2O_4$/PZT composite ceramics. Yttrium-iron garnet ($Y_3Fe_5O_{12}$ or YIG [45,50]) also possesses a small value of K_m^2. It is worth noting that large magnetoelectric coefficients have been observed for YIG [13].

Table 1. The material characteristics of piezomagnetic cubic crystals of class $m3m$. Note that the magnetic permeability of a vacuum is $\mu_0 = 4\pi \times 10^{-7}$ [$H \times m^{-1}$] $\sim 12.566371 \times 10^{-7}$ [$(V \times s) \times (A \times m)^{-1}$] and Tesla $= N \times (A \times m)^{-1}$.

Crystal	C_{44}, 10^{10} N/m^2	h_{16}, Tesla	μ_{11}, 10^{-6} N/A^2	ρ, kg/m^3	K_m^2, %	K_m	a_{Km}	μ_{11}/μ_0
Ni	13.090	384.240	26.46792	8914	4.2613	0.20643	0.82017	21.06250
Alfenol	12.300	824.627	66.85795	7848	8.2691	0.28756	0.93064	53.20387
Terfenol-D(1)	0.610	97.119	2.74889	7800	56.2498	0.75000	1.22474	2.18750
Terfenol-D(2)	0.610	28.160	6.28300	9060	2.0690	0.14384	0.70606	4.99985
Terfenol-D(3)	0.610	217.360	3.34200	9060	231.7517	1.52234	1.34949	2.65948
Ferroxcube 7A1	8.970	417.565	23.19315	7890	8.3810	0.28950	0.93290	18.45652
Metglas 2605	10.447	28,367.248	>9550.0	7180	80.6565	0.89809	1.26577	>7600.0
$NiFe_2O_4$	8.120	96.700	25.13274	5370	0.4582	0.06769	0.50304	20.00000
$Ni_{0.8}Zn_{0.2}Fe_2O_4$	8.120	125.700	25.13274	5370	0.7742	0.08799	0.56776	20.00000
YIG	7.640	119.000	15.07964	5370	1.2292	0.11087	0.63010	12.00000

5. Results of calculations and discussion

Table 2 lists the SH-SAW characteristics for the cubic piezomagnetic monocrystals. First of all, the important characteristic such as the velocity V_{aKm} is calculated for the cubic crystals because the true SH-SAW velocity, namely the USZW velocity for piezomagnetics with $K_m^2 > 1/3$ is computed just below the V_{aKm}, but not just below the velocity V_{tm} of the bulk SH-wave. It is thought that the third Terfenol-D in the table is a good example for the case of $K_m^2 > 1/3$, because the USZW velocity V_{USZWc} is only ~ 0.25 m/s slower that the V_{aKm} but several hundred meters per second slower than the V_{tm}. Notwithstanding, Terfenol-D(3) with $K_m^2 \sim 2.32$ has 1% smaller value of K^2 in the table seventh column compared with Terfenol-D(1) with $K_m^2 \sim 0.56$. This demonstrates a complicated dependence of the USZW velocity V_{USZWc} on the value of K_m^2. It is necessary to mention the well-known opinion in the research community such that $K_m^2 < 1$ must occur for a right set of material constants. However, Terfenol-D(3) with $K_m^2 \sim 2.32$ is a good example material for comparison with Terfenol-D(1) with $K_m^2 \sim 0.56$ to indicate that Terfenol-D(1) is more preferable. It is also noted that the difference for Terfenol-D(1) is approximately 9 m/s between the velocities V_{USZWc} and V_{aKm} and is more than 7 m/s between the velocities V_{BGc} and V_{tm}. This manifests that the USZW velocity in some apt cubic piezomagnetics can be significantly smaller than the V_{aKm}. Also, it is thought that the value of $(V_{tm} - V_{BGc}) \sim 7$ m/s for Terfenol-D(1) represents a good present for experimentalists. Such material like Terfenol-D(1) allows one to have an attempt to find an answer to the following question: what is the surface BG-wave, an instability of the bulk SH-wave or the SH-SAW and SH-BAW are independent in the transversely-isotropic piezomagnetics? For this purpose, it is noted that the improved optical method for measurements of both the phase and group velocities described in [51] allows one to measure the phase velocity with an accuracy $\sim$2 m/s. Also, an interesting result given in Table 2 was obtained for Metglas with $K_m^2 > 1/3$. Indeed, these piezomagnetics can be used as matrices to form piezoelectromagnetics. It is possible that the reader is already familiar with recent book [52] by the author published in 2011 concerning the wave propagation problem in proposed cubic piezoelectromagnetics.

For piezomagnetics Ni and Alfenol with $K_m^2 < 1/3$, the USZW velocity V_{USZWc} also significantly differs from the surface BG-wave velocity V_{BGc} calculated with the well-known formula given in the title of Table 2. According to the last two columns of the table, the difference between the values of $(V_{tm} - V_{USZWc})$ and $(V_{tm} - V_{BGc})$ is observed already in the first non-zero digit after the decimal point, and the first value for Alfenol is approximately 1.5 times larger than the second. However, for the piezomagnetics $NiFe_2O_4$, $Ni_{0.8}Zn_{0.2}Fe_2O_4$, and YIG with a very small values of $K_m^2 \ll 1/3$ in Table 2, the values of $(V_{tm} - V_{USZWc})$ and $(V_{tm} - V_{BGc})$ differ from each other in the second non-zero digit after the decimal point.

It is thought that it is indispensable to graphically demonstrate SH-SAW solutions for both cases of $K_m^2 < 1/3$ and $K_m^2 > 1/3$. Figure 2 shows the behavior of the boundary-condition determinant (BCD2) for Alfenol with $K_m^2 < 1/3$; see Table 1. Indeed, the solution is found just below the velocity V_{tm} of the bulk SH-wave.

On the other hand, Figure 3 shows the BCD2 behavior for such well-known metal as Terfenol-D(1) with $K_m^2 > 1/3$. This is nearly ideal example because the case can demonstrate solutions of the velocities V_{tm}, V_{USZWc}, and V_{USZWo} situated near

Table 2. The wave characteristics of piezomagnetic cubic crystals of class $m3m$. The velocity V_{aKm} is calculated using Equation (19). Noted that the SAW velocity V_{USZWc} listed in this table for the piezomagnetics differs from the Bleustein–Gulyaev wave velocity calculated with the following well-known formula: $V_{BGc} = V_{tm}\{1-(K_m^2/[(1+K_m^2)\times(1+\mu_{11}/\mu_0)])^2\}^{1/2}$, where $\mu_0 = 4\pi\times10^{-7}$ [N/A^2]; $V_{USZWo} = V_{BGo} = V_{tm}\{1-(K_m^2/[(1+K_m^2)])^2\}^{1/2}$. Note that $K^2 = 2(V_{USZWc} - V_{USZWo})/V_{USZWc}$, $\Delta_{ZW} = V_{tm} - V_{USZWc}$ and $\Delta_{BG} = V_{tm} - V_{BGc}$.

Crystal	V_{aKm}, m/s	V_{t4}, m/s	V_{tm}, m/s	V_{USZWc}, m/s	V_{USZWo}, m/s	K^2, %	Δ_{ZW}, m/s	Δ_{BG}, m/s
Ni	3142.943875	3832.070660	3912.867571	3912.859614	3909.597995	0.17	0.007957	0.006714
Alfenol	3684.295642	3958.886569	4119.317545	4119.311710	4107.285623	0.58	0.005835	0.004089
Terfenol-D(1)	1083.086428	884.336634	1105.420187	1074.169296	1031.304608	7.98	31.250891	7.072821
Terfenol-D(2)	579.355121	820.542006	828.987208	828.982134	828.816870	0.04	0.005074	0.004731
Terfenol-D(3)	1107.311991	820.542006	1494.539548	1107.057627	1069.405746	6.80	387.481921	27.483376
Ferroxcube 7A1	3145.532839	3371.768273	3510.219727	3510.180568	3499.708808	0.60	0.039159	0.027724
Metglas 2605	4828.238151	3814.464481	5126.965411	4828.238150	4587.618479	9.97	298.727261	0.000009
$NiFe_2O_4$	1956.129067	3888.578510	3897.477102	3897.477008	3897.436560	0.002	0.000094	0.000092
$Ni_{0.8}Zn_{0.2}Fe_2O_4$	2207.786872	3888.578510	3903.602920	3903.602649	3903.487709	0.006	0.000271	0.000261
YIG	2376.656277	3771.894495	3795.005066	3795.003333	3794.725293	0.015	0.001733	0.001655

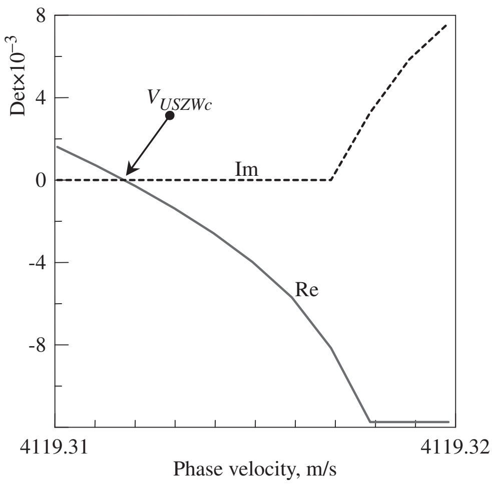

Figure 2. The behavior of the boundary-condition determinant (BCD2) for Alfenol with $K_m^2 < 1/3$. The solution for the V_{USZWc} (see also Table 2) is demonstrated.

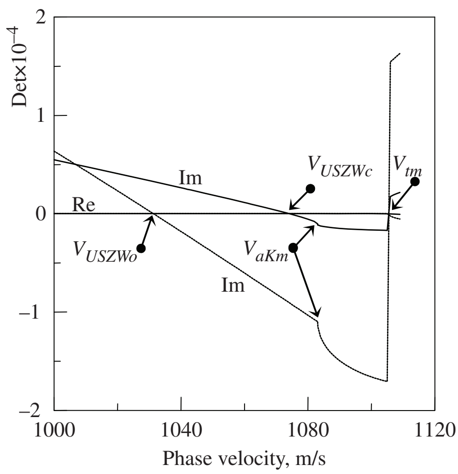

Figure 3. The behavior of the boundary-condition determinants (BCD2) for Terfenol-D(1) with $K_m^2 > 1/3$. The dotted lines are for the BCD2 behavior in the case of $\psi = 0$. Three solutions for V_{tm}, V_{USZWc}, and $V_{USZWo} = V_{BGo}$ (see also Table 2) are demonstrated.

each other. It is clearly seen in Figure 3 that linear dependencies of the BCD2 on the V_{ph} occur below the velocity V_{aKm}; see the solid and dotted lines in the figure.

Figures 4 and 5 show the dependence of the eigenvalues and eigenvector components for Terfenol-D(1) on the V_{ph} in the vicinity of the velocity V_{aKm}.

It is thought that any knowledge of ultrasonic characteristics can be useful for choice of suitable materials (metals) for various smart devices in the microwave technology. Also there are many nondestructive techniques for some suitable characterizations of smart devices and they are continuously developed and improved. For instance, Potter and Dixon [53] demonstrated a comparison of

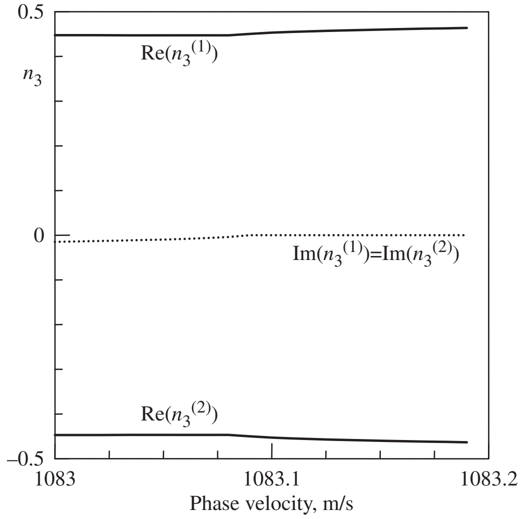

Figure 4. The dependence of the eigenvalues $n_3^{(1)}$ and $n_3^{(2)}$ on the phase velocity V_{ph} for Terfenol-D(1) near the V_{aKm} (see also Table 2).

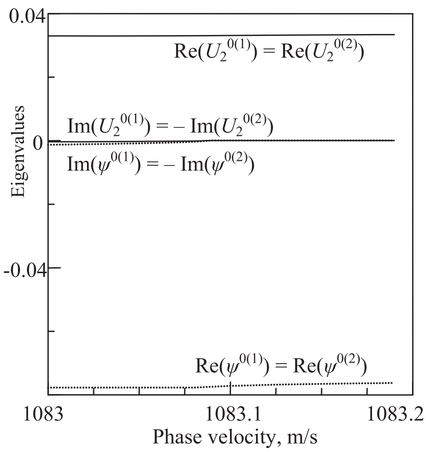

Figure 5. The dependence of the eigenvectors $(U_2^{0(1)}, \psi^{0(1)})$ for $n_3^{(1)}$ and $(U_2^{0(2)}, \psi^{0(2)})$ for $n_3^{(2)}$ on the phase velocity V_{ph} for Terfenol-D(1) near the V_{aKm} (see also Table 2).

Lamb and shear wave techniques for the ultrasonic evaluation of the crystallographic texture of steel metals. Note that metals can frequently possess crystallographic cubic structure. For the shear wave technique, polarized shear waves through thickness mode were used. This can allow the determination of additional material parameters such as the material thickness. Also, EMATs can be used for ultrasonic detection and ultrasonic generation of both types of waves. Through-thickness shear waves can be generated by driving an EMAT with a broadband pulse of peak frequency ~4.5 MHz [53].

Finally, it is possible to discuss SAW devices and fabrication techniques for them, for instance, see the works cited in [54–56]. The patents [54] contain further references on the subject and describe devices disclosed for controlling high frequency (optic or electric) signals by the generation of SH-SAWs, for instance, the surface BG-wave. The number of devices requiring frequency control has grown in number and complexity. Also there is a commensurate growth of requirements for controlling higher frequencies desirable for microwave generators and high definition television. The SAW devices [54] can use certain bulk or surface-modified crystalline substrates which have a surface with a receiving area and an input interdigital transducer (IDT) deposited on the signal receiving area of the substrate surface. The used materials can support the BG wave propagation with the phase velocities ~4000 m/s and ~5000 m/s. It is well-known that the BG wave is non-dispersive, as well as the SH-SAWs studied in this work. This means that the phase velocity is equal to the group velocity and defined by the formula written above after Equation (12): $v_{ph} = \omega/k = \nu\lambda$ where $\omega = 2\pi\nu$ and $k = 2\pi/\lambda$, ν and λ are the linear frequency and wavelength, respectively. SH-SAWs were generated and the transmission data for the device were also monitored in [54] using a commercially available network analyzer. A large transmission peak center was observed at ~252 MHz for the used wavelength of ~16 μm. This gives ~4000 m/s for the calculated velocity of this acoustic wave mode which agrees with the theoretically calculated value. The transmission data [54] also showed that other acoustic wave modes were simultaneously generated. One of them (peak center at 360 MHz) possessed higher speed than SAW and can relate to a kind of bulk acoustic wave. The patents [54] also describe an example of the SAW generation having $\lambda/2$ (i.e. 2ν) of the SAW generated by utilizing a hydrothermally-grown z-cut KTP crystal having ferroelectric domains reversed under the IDT. Transmission data of the resulting device shows a large transmission peak centers at ~504 MHz for the wavelength of ~8 μm. This also gives the SAW propagation speed of ~4000 m/s. This illustrates that one can obtain double the frequency for the same IDT design by using domain reversal on the area of the KTP substrate to which the input IDT is applied. This exemplifies that the frequency can be increased by using a suitable wavelength to keep the same propagation speed for the non-dispersive SH-SAWs. Therefore, it is usual to give the dependencies on the phase velocity V_{ph} in Figures 2–5 (see also Table 2) because the frequency can depend on experimental patterns. Using the calculated data listed in Table 2, one can state that for higher frequencies, it is possible that all cubic material, but Terfenol-D, can be suitable because they have the speed ~4000 m/s or higher. It is thought that the most promising material of them is Metglas because it can possess the largest coupling coefficient.

6. Conclusion

This report demonstrates results concerning characteristics of the shear-horizontal surface acoustic waves (SH-SAWs) propagating in direction [101] in cubic piezomagnetics. The cubic piezomagnetics are well-known and used in smart materials during the last half-century, and, therefore, promising cubic piezomagnetic materials were studied. Some of the studied cubic piezomagnetics can possess the coefficient of the magnetomechanical coupling $K_m^2 < 1/3$ and some of them such as

Terfenol-D and Metglas can have $K_m^2 > 1/3$. Materials with $K_m^2 > 1/3$ demonstrate the SH-SAW propagation with the phase velocity slightly below the velocity V_{aKm} where the value of V_{aKm} can be significantly smaller than that of V_{tm} for $K_m^2 \to 1$. It is thought that this knowledge can be useful for choice of likely materials for various smart devices in microwave technology. Also, cubic piezomagnetics or cubic piezoelectromagnetic composite materials can be exploited instead of hexagonal ($6\,mm$) materials [57].

Acknowledgements

The author would like to thank all the referees for their great interest in this theoretical work, useful notes, and fruitful discussions. It is also necessary to greatly thank Professor X.-F. Li from the Institute of Mechanics and Sensor Technology, School of Civil Engineering and Architecture, Central South University, Changsha, Hunan, China, for very fruitful discussions and support of this work.

References

[1] J.L. Bleustein, *A new surface wave in piezoelectric materials*, Appl. Phys. Lett. 13 (1968), pp. 412–413.
[2] Yu.V. Gulyaev, *Electroacoustic surface waves in solids*, JETP Lett. 9 (1969), pp. 37–38.
[3] V.I. Al'shits, A.N. Darinskii, and J. Lothe, *On the existence of surface waves in half-infinite anisotropic elastic media with piezoelectric and piezomagnetic properties*, Wave Motion 16 (1992), pp. 265–283.
[4] Yu.V. Gulyaev and F.S. Hickernell, *Acoustoelectronics: History, present state and new ideas for a new era*, Acoust. Phys. 51 (2005), pp. 81–88.
[5] A.A. Zakharenko, *New solutions of shear waves in piezoelectric cubic crystals*, J. Zhejiang Univ. Sci. A 8 (2007), pp. 669–674.
[6] A.A. Zakharenko, *First evidence of surface SH-wave propagation in cubic piezomagnetics*, J. Electromagn. Anal. Appl. 2 (2010), pp. 287–296.
[7] Y. Huang, X.-F. Li, and K.Y. Lee, *Interfacial shear horizontal (SH) waves propagating in a two-phase piezoelectric/piezomagnetic structure with an imperfect interface*, Phil. Mag. Lett. 89 (2009), pp. 95–103.
[8] C.C. Tseng, *Piezoelectric surface waves in cubic crystals*, J. Appl. Phys. 41 (1970), pp. 2270–2276.
[9] C.C. Tseng, *Piezoelectric surface waves in cubic and orthorhombic crystals*, Appl. Phys. Lett. 16 (1970), pp. 253–255.
[10] G. Koerber and R.F. Vogel, *Generalized Bleustein modes*, IEEE Trans. Son. Ultrason. SU-19 (1972), pp. 3–8.
[11] V.M. Bright and W.D. Hunt, *Bleustein–Gulyaev waves in gallium arsenide and other piezoelectric cubic crystals*, J. Appl. Phys. 66 (1989), pp. 1556–1564.
[12] A.A. Zakharenko, *Propagation of Seven New SH-SAWs in Piezoelectromagnetics of Class 6mm*, LAP Lambert Academic Publishing, Saarbruecken-Krasnoyarsk, 2010.
[13] M. Fiebig, *Revival of the magnetoelectric effect*, J. Phys. D: Appl. Phys. 38 (2005), pp. R123–R152.
[14] J. Zhai, Z.-P. Xing, S.-X. Dong, J.-F. Li, and D. Viehland, *Magnetoelectric laminate composites: An overview*, J. Am. Ceram. Soc. 91 (2008), pp. 351–58.
[15] J. Ryu, S. Priya, K. Uchino, and H.-E. Kim, *Magnetoelectric effect in composites of magnetostrictive and piezoelectric materials*, J. Electroceram. 8 (2002), pp. 107–119.

[16] J. van Suchtelen, *Product properties: A new application of composite materials*, Philips Res. Rep. 27 (1972), pp. 28–37.
[17] J. van den Boomgaard, D.R. Terrell, R.A.J. Born, and H.F.J.I. Giller, *In-situ grown eutectic magnetoelectric composite-material. 1. Composition and unidirectional solidification*, J. Mater. Sci. 9 (1974), pp. 1705–1709.
[18] A.M.J.G. van Run, D.R. Terrell, and J.H. Scholing, *In-situ grown eutectic magnetoelectric composite-material. 2. Physical properties*, J. Mater. Sci. 9 (1974), pp. 1710–1714.
[19] J. van den Boomgaard, A.M.J.G. van Run, and J. van Suchtelen, *Piezoelectric–piezomagnetic composites with magnetoelectric effect*, Ferroelectrics 14 (1976), pp. 727–728.
[20] V.E. Wood and A.E. Austin, *Possible applications for magnetoelectric materials*, in *Magnetoelectric Interaction Phenomena in Crystals*, A.J. Freeman and H. Schmid, eds., Gordon and Breach Science Publishers, Newark, NJ, 1975, pp. 181–194.
[21] M. Avellaneda and G. Harshe, *Magnetoelectric effect in piezoelectric/magnetostrictive multilayer (2-2) composites*, J. Intell. Mater. Syst. Struct. 5 (1994), pp. 501–513.
[22] S. Srinivas, J.Y. Li, Y.C. Zhou, and A.K. Soh, *The effective magnetoelectroelastic moduli of matrix-based multiferroic composites*, J. Appl. Phys. 99 (2006), 043905.
[23] C.W. Nan, *Magnetoelectric effect in composites of piezoelectric and piezomagnetic phases*, Phys. Rev. B: Condens. Matter 50 (1994), pp. 6082–6088.
[24] P. Yang, K. Zhao, Y. Yin, J.G. Wan, and J.S. Zhu, *Magnetoelectric effect in magnetostrictive/piezoelectric laminate composite Terfenol-D/LiNbO$_3$ [(zxtw)−129°/30°]*, Appl. Phys. Lett. 88 (2006), p. 172903.
[25] K. Mori and M. Wuttig, *Magnetoelectric coupling in Terfenol-D/polyvinylidene difluoride composites*, Appl. Phys. Lett. 81 (2002), pp. 100–101.
[26] M.I. Bichurin, D.A. Filippov, V.M. Petrov, V.M. Laletsin, N. Paddubnaya, and G. Srinivasan, *Resonance magnetoelectric effects in layered magnetostrictive-piezoelectric composites*, Phys. Rev. B: Condens. Matter 68 (2003), p. 132408.
[27] J. Chen, E. Pan, and H. Chen, *Wave propagation in magneto-electro-elastic multilayered plates*, Int. J. Solid Struct. 44 (2007), pp. 1073–1085.
[28] Ü. Özgür, Ya. Alivov, and H. Morkoç, *Microwave ferrites, part 2: Passive components and electrical tuning*, J. Mater. Sci.: Mater. Electron. 20 (2009), pp. 911–952.
[29] G. Srinivasan, *Magnetoelectric composites*, Annu. Rev. Mater. Res. 40 (2010), pp. 153–178.
[30] A.-K. Soh and J.-X. Liu, *Interfacial shear horizontal waves in a piezoelectric–piezomagnetic bi-material*, Phil. Mag. Lett. 86 (2006), pp. 31–35.
[31] J.N. Nye, *Physical Properties of Crystals. Their Representation by Tensors and Matrices*, Clarendon Press, Oxford, 1989.
[32] R.E. Newnham, *Properties of Materials: Anisotropy, Symmetry, Structure*, Oxford University Press, USA, 2004, 392 pp.
[33] V.E. Lyamov, *Polarization Effects and Interaction Anisotropy of Acoustic Waves in Crystals*, MSU Publishing, Moscow, 1983 (in Russian).
[34] G.W. Farnell and E.L. Adler, *Elastic wave propagation in thin layers*, in *Physical Acoustics: Principles and Methods*, Vol. 9, W.P. Mason and R.N. Thurston, eds., Academic Press, New York, 1972, pp. 35–127.
[35] A.A. Zakharenko, *On cubic crystal anisotropy for waves with Rayleigh-wave polarization*, Nondestr. Test. Eval. 21 (2006), pp. 61–77.
[36] R.C. Hall, *Single crystal anisotropy and magnetostriction constants of several ferromagnetic materials including alloys of NiFe, SiFe, AlFe, CoNi, and CoFe*, J. Appl. Phys. 30 (1959), pp. 816–819.
[37] H.J. Leamy, E.D. Gibson, and F.X. Kayser, *The elastic stiffness constants of iron–aluminum alloys. I. Experimental results and thermodynamic analysis*, Acta Metall. Mater 15 (1967), pp. 1827–1838.

[38] Z. Kaczkowski, *Effect of a magnetic field on the piezomagnetic parameters of some magnetostrictive materials*, Ultrasonics 8 (1970), pp. 239–242.
[39] I.J. Busch-Vishniac, *Electromechanical Sensors and Actuators*, Springer-Verlag, New York, 1999, p. 186.
[40] W.P. Mason, *Physical Acoustics and the Properties of Solids*, Van Nostrand, Princeton, NJ, 1958.
[41] W.P. Mason, *Crystal Physics of Interaction Processes*, Academic Press, New York, 1966.
[42] Ya.T. Shah, A.B. Pandit, and V.S. Moholkar, *Cavitation Reaction Engineering*, Kluwer Academic/Plenum Publishers, New York, 1999, p. 278.
[43] J. Zhai, Sh. Dong, Z. Xing, J. Li, and D. Viehland, *Giant magnetoelectric effect in Metglas/polyvinylidene fluoride laminates*, Appl. Phys. Lett. 89 (2006), p. 083507.
[44] A.E. Giannakopoulos and A.Z. Parmaklis, *The contact problem of a circular rigid punch on piezomagnetic materials*, Int. J. Solid Struct. 44 (2007), pp. 4593–4612.
[45] M.I. Bichurin, I.A. Kornev, V.M. Petrov, A.S. Tatarenko, Yu.V. Kiliba, and G. Srinivasan, *Theory of magnetoelectric effects at microwave frequencies in a piezoelectric/magnetostrictive multilayer composite*, Phys. Rev. B: Condens. Matter 64 (2001), p. 094409.
[46] V.M. Petrov and G. Srinivasan, *Enhancement of magnetoelectric coupling in functionally graded ferroelectric and ferromagnetic bilayers*, Phys. Rev. B: Condens. Matter 78 (2008), p. 184421.
[47] H. Liu, S.N. Zhu, Z.G. Dong, Y.Y. Zhu, Y.F. Chen, N.B. Ming, and X. Zhang, *Coupling of electromagnetic waves and superlattice vibrations in a piezomagnetic superlattice: creation of a polariton through the piezomagnetic effect*, Phys. Rev. B: Condens. Matter 71 (2005), p. 125106.
[48] J. Zhai, N. Cai, Zh. Shi, Yu. Lin, and C.-W. Nan, *Coupled magnetodielectric properties of laminated* $PbZr_{0.53}Ti_{0.47}O_3/NiFe_2O_4$ *ceramics*, J. Appl. Phys. 95 (2004), pp. 5685–5690.
[49] J. Zhai, N. Cai, Zh. Shi, Yu. Lin, and C.-W. Nan, *Magnetic–dielectric properties of* $NiFe_2O_4$*/PZT particulate composites*, J. Phys. D: Appl. Phys. 37 (2004), pp. 823–827.
[50] V.M. Petrov, V.V. Zibtsev, and G. Srinivasan, *Magnetoacoustic resonance in ferrite-ferroelectric nanopillars*, Eur. Phys. J. B 71 (2009), pp. 367–370.
[51] E.A. Kolosovskii, A.V. Tsarev, and I.B. Yakovkin, *Improved procedure for measuring SAW velocity in anisotropic structures*, Acoust. Phys. 44 (1998), pp. 793–800.
[52] A.A. Zakharenko, *Seven New SH-SAWs in Cubic Piezoelectromagnetics*, LAP Lambert Academic Publishing, Saarbruecken-Krasnoyarsk, 2011.
[53] M.D.G. Potter and S. Dixon, *Ultrasonic texture measurement of sheet metals: An integrated system combining Lamb and shear wave techniques*, Nondestr. Test. Eval. 20 (2005), pp. 201–210.
[54] D.K.-T. Chu, *Acoustic wave devices for controlling high frequency signals*, US Patent 5350961, September 27, 1994; D.K.-T. Chu and W.Y.-H. Hsu, *Acoustic wave devices for controlling high frequency signals*, WO Patent 1994003972, February 17, 1994.
[55] H.I. Smith, *Fabrication techniques for surface-acoustic-wave and thin-film optical devices*, Proc. IEEE 62 (1974), pp. 1361–1387.
[56] H.I. Smith, *Acoustic surface waves: Fabrication techniques for surface wave devices*, Top. Appl. Phys. 24 (1978), pp. 305–324.
[57] A.A. Zakharenko, *Twenty-two New Interfacial SH-Waves in Dissimilar PEMS*, LAP Lambert Academic Publishing, Saarbruecken-Krasnoyarsk, 2012.